Radical transfer but not heme distal residues is essential for pH dependence of dye-decolorizing activity of peroxidase from *Vibrio cholerae*

Takeshi Uchida,*[a,b] Issei Omura,[b] Sayaka Umetsu,[b] and Koichiro Ishimori[a,b]

[a]Department of Chemistry, Faculty of Science, Hokkaido University, Sapporo 060-0810, Japan

[b]Graduate School of Chemical Sciences and Engineering, Hokkaido University, Sapporo 060-8628, Japan

*Corresponding author: Department of Chemistry, Faculty of Science, Hokkaido University, Sapporo 060-0810, Japan

E-mail address: uchida@sci.hokudai.ac.jp (T. Uchida).

Keywords: heme, enzyme, peroxidase, reaction mechanism, dye-degradation, *Vibrio cholerae*

ABSTRACT

Dye-decolorizing peroxidase (DyP) is a heme-containing enzyme that catalyzes the degradation of anthraquinone dyes. A main feature of DyP is the acidic optimal pH for dye-decolorizing activity. In this study, we constructed several mutant DyP enzymes from *Vibrio cholerae*, with a view to identifying the decisive factor of the low pH preference of DyP. Initially, distal Asp144, a conserved residue, was replaced with His, which led to significant loss of dye-decolorizing activity. Introduction of His into a position slightly distant from heme resulted in restoration of activity but no shift in optimal pH, indicating that distal residues do not contribute to the pH dependence of catalytic activity. His178, an essential residue for dye decolorization, is located near heme and forms hydrogen bonds with Asp138 and Thr277. While Trp and Tyr mutants of His178 were inactive, the Phe mutant displayed ~35% activity of wild-type *Vc*DyP, indicating that this position is a potential radical transfer route from heme to the active site on the protein surface. The Thr277Val mutant displayed similar enzymatic properties as WT *Vc*DyP, whereas the Asp138Val mutant displayed significantly increased activity at pH 6.5. On the basis of these findings, we propose that neither distal amino acid residues, including Asp144, nor hydrogen bonds between His178 and Thr277 are responsible while the hydrogen bond between His178 and Asp138 plays a key role in the pH dependence of activity.

1. Introduction

Dye-decolorizing peroxidase (DyP) (EC 1.11.1.19) is a member of the heme-containing peroxidase family that catalyzes oxidation of substrates using hydrogen peroxide, H_2O_2, as an electron acceptor. Although the specific biological functions of DyPs are unknown at present, the enzymes have been shown to catalyze degradation of anthraquinone dyes [1,2]. DyP enzymes were initially discovered in fungi followed by several bacterial counterparts. In view of the finding that the genomic sequence of *Vibrio cholerae* contains a gene (VC2145) encoding potential B-type DyP, we previously constructed a system for VC2145 expression in *Escherichia coli* [3]. The purified protein possessed similar dye-decolorizing activity as other known DyPs [4–6]. In the majority of heme peroxidases, histidine located in the heme distal site functions as an acid-base catalyst [7]. In addition, distal arginine plays a key role in forming an oxoferryl porphyrin cation radical (compound I) [8–11], which is transferred to the protein surface to react with substrates [12–15]. The crystal structure of DyP (VC2145) from *V. cholerae* (*Vc*DyP) revealed the presence of two charged residues, Asp144 and Arg230, that are conserved in most DyPs (Fig. 1) [9,16,17], but no histidine in the heme distal pocket [3].

A prominent feature of the DyP family is the extremely low pH preference for enzymatic activity [18]. Dye decolorization by DyP is strongly pH-dependent, with optimal activity at pH of ~4. This low pH value is believed to be attributable to the presence of a distal aspartic acid (Asp144 for *Vc*DyP), since the pK_a value of the side-chain of this residue in water is 3.9 [19]. The distal aspartic acid is proposed to act as a general acid-base catalyst in the DyP reaction as reported for chloroperoxidase (CPO) [20].

In this study, we investigated the origin of the pH dependence of dye-decolorizing activity. Since distal residues in the heme binding site are a possible determinant, histidine was introduced into the heme distal site in lieu of Asp144, Leu244 and Phe246 of *Vc*DyP, with the intention of shifting the optimal pH of the dye-decolorizing reaction. The pH profiles of all the

mutants examined were altered only slightly, indicating that distal charged residues do not contribute to pH dependence of the dye-decolorizing activity of *Vc*DyP. His178, which is located near heme and within a hydrogen bonding distance to Asp138 and Thr277, is essential for dye decolorization [3]. Notably, mutation of Thr277 to valine did not affect pH dependence while mutation of Asp138 to valine led to a ~10-fold increase in enzymatic efficiency at pH 8.0. Our collective results clearly support the involvement of the hydrogen bond between His178 and Asp138 in the pathway of radical transfer to the protein surface, resulting in pH-dependent catalytic activity.

2. Experimental section

2.1. Materials

All chemicals were purchased from Wako Pure Chemical Industries (Osaka, Japan), Nacalai Tesque (Kyoto, Japan), Kanto Chemical (Tokyo, Japan) or Sigma-Aldrich (St. Louis, MO, USA), and used without further purification.

2.2. Protein expression and preparation

DyP proteins were expressed and purified as described previously [3]. Briefly, DyP-containing plasmid with the His_6 tag was expressed in *Escherichia coli* BL21(DE3) cells cultured in M9 minimal medium supplemented with 50 μg mL^{-1} kanamycin to suppress protein-bound protoporphyrin IX levels. Protein isolation was performed using HisTrap HP column chromatography (GE Healthcare, Uppsala, Sweden). After reconstitution of protein with an equimolar amount of heme (1:1), the sample was applied to a gel filtration column (HiLoad 16/60 Superdex 200 pg; GE Healthcare) equilibrated with 50 mM Tris-HCl and 150 mM NaCl (pH 8.0). Purity was confirmed as >90% via SDS-PAGE.

Mutagenesis was conducted utilizing the PrimeSTAR mutagenesis basal kit from Takara Bio (Otsu, Japan) using wild-type expression vector as the template. DNA oligonucleotides were purchased from Eurofins Genomics (Tokyo, Japan). Genes were sequenced (Eurofins

Genomics, Tokyo, Japan) to ensure that only the desired mutations were introduced. The primers employed for mutation are listed in Supplemental Table S1.

2.3. Dye-decolorizing assay

Dye-decolorization activity was determined by spectrophotometric measurement of the rate of H_2O_2-mediated decomposition of Reactive blue 19 (RB19). Briefly, 900 μL hemin-reconstituted protein solution (final concentration of 0.3 μM unless specified otherwise) was placed in a 1 mL cuvette along with 10–50 μL substrate solution for testing. The reaction was initiated by the addition of 100 μL of 2 mM H_2O_2 (final conc. 0.2 mM) in the same buffer with incubation for 3 min at 25 °C. The substrate concentration was measured at 595 nm (ε_{595} = 10 mM^{-1} cm^{-1}) using a V-660 spectrophotometer (Jasco, Tokyo, Japan). H_2O_2 concentrations were determined spectrophotometrically using a molar extinction coefficient of 43.6 $M^{-1}cm^{-1}$ at 240 nm [21]. The pH profile of dye-decolorizing activity was assessed by measuring the specific activity, which was calculated by measuring the decrease in absorbance at 595 nm 100 s after initiating the reaction [22]. Kinetic parameters (V_{max} and K_M) were assessed by fitting the initial rate (v_0) against substrate concentration ([S]) to the Michaelis-Menten equation as follows:

$$v_0 = \frac{V_{max}[S]}{K_M + [S]} \quad (1)$$

The turnover number (k_{cat}) was obtained by dividing V_{max} by the enzyme concentration.

2.4. Reaction with H_2O_2

Compound I formation via reaction with H_2O_2 was monitored with a stopped-flow apparatus (Unisoku, Osaka, Japan) by following the decrease in absorbance at 406 nm. In a typical experiment, one syringe contained 10 μM DyP (50 mM citrate at pH 4.0 or 100 mM Na-Pi at pH 7.0) and another contained the corresponding buffer with 10 μM H_2O_2.

3. Results

3.1. Introduction of histidine into the heme distal pocket

Asp144 located in the heme pocket (Fig. 1) and conserved in the DyP family is proposed to perform an essential peroxidase function in DyP from *V. cholerae* (*Vc*DyP) based on the finding that its replacement with valine leads to almost complete loss of dye-decolorization activity [3]. This result suggests that distal aspartic acid (Asp144) acts as an acid-base catalyst, as observed for other DyP enzymes [9,10]. The optimal pH of peroxidases is proposed to be potentially associated with residues at the heme distal site [23,24]. In our experiments, Asp144 was initially replaced with histidine (pK_a 6.0) (D144H), with the aim of altering the optimal pH of the dye-decolorizing activity of *Vc*DyP towards a neutral value. The purified D144H mutant reconstituted with hemin displayed a similar absorption spectrum as wild-type (WT) *Vc*DyP (Supplemental Fig. S1A) [3]. The Soret maximum appeared at 406 nm. However, the presence of a small shoulder at 388 nm probably due to free heme indicated a slight reduction in affinity of the D144H mutant for heme. Next, dye-decolorizing activity was monitored using Reactive blue 19 (RB19) as a substrate. The time-course of absorbance changes at 595 nm in the reaction with hydrogen peroxide (H_2O_2) at pH 4.0 is presented in Fig. 2. Almost no absorbance change at 595 nm was observed for the D144H mutant at pH 4.0 after initiation of the reaction, indicating drastic loss of enzymatic activity. The circular dichroism (CD) spectrum of the D144H mutant at pH 4.0 was similar to that of WT *Vc*DyP, suggesting that denaturation of the protein owing to mutation is not a direct cause of loss of activity (Supplemental Fig. S2). Although the D144H mutant was expected to be inactive at pH 4.0 owing to the substitution, inactivation at pH 7.0 (Fig. 2, green line) was unexpected, since the introduced histidine was presumed to function as an acid-base catalyst at neutral pH. Our results led to the conclusion that histidine at position 144 cannot act as an acid-base catalyst at any pH.

Previous studies on peroxidase and peroxygenase activities of mutant myoglobin have demonstrated that distal histidine functions as an acid-base catalyst only when located at a suitable position [25–27]. The closest proximity between His144 and heme iron in D144H mutant *Vc*DyP was estimated as 4.1 Å (Fig. 3A), similar to that in myoglobin (4.0 Å) [28]. In

this case, His144 was located too close to the heme iron to function as an acid-base catalyst. Accordingly, we designed two double mutants (D144V/L244H and D144V/F246H) in which Asp144 was replaced with valine and histidine was introduced into heme distal sites slightly distant from the heme iron in relation to the D144H mutant. On the basis of the crystal structure of WT *Vc*DyP [3], distances between the heme iron and side-chain of the introduced histidine in the D144V/L244H and D144V/F246H mutants were estimated as 7.2 and 5.4 Å, respectively (Fig. 3B, C).

The Soret maximum of both mutants was 406 nm (Supplemental Fig. S1A), which was equivalent to that of WT *Vc*DyP. The Soret band of the D144V/F246H mutant was comparable with that of WT *Vc*DyP whereas that of the D144V/L244H mutant displayed a shoulder at 388 nm. This shoulder remained after gel filtration, indicating that introduction of histidine at position 244 into the D144V mutant affects heme coordination and reduces the affinity for heme. However, considering the similarities of the CD spectra of D144V/L244H and D144V/F246H mutants (Supplemental Fig. S2), the secondary structure of the protein did not appear altered by the additional mutation. The time courses of absorbance changes at 595 nm for D144V/L244H and D144V/F246H mutants at pH 4.0 were slower than that of WT *Vc*DyP but significantly faster than that of the D144H mutant (Fig. 2A). While the D144H mutant was almost completely inactive (Fig. 2A), introduction of histidine at an appropriate position led to restoration of dye decolorization activity. Appropriate distance between histidine and the distal oxygen of the heme-bound hydroperoxide is essential for efficient heterolytic cleavage of the O-O bond, as specified in the Discussion section.

The pH profiles of the activities of WT, D144V/L244H and D144V/F246H mutant *Vc*DyP were examined (Fig. 2B) and compared based on the amount of substrate (RB19) degraded in the reaction with H_2O_2 at 25 °C for 100 s. For WT *Vc*DyP, activity was highest at pH 4.5 and decreased with increasing pH from 4.5 to 7.0, almost reaching a plateau at pH > 7.0 (Fig. 2B, black). The pH profile of the D144V/L244H mutant showed optimal activity at pH 4.0 (Fig. 2B,

red), indicating that the introduction of histidine led to lowering of optimal pH by 0.5 (Supplemental Table S2). A similar trend was observed for the D144V/F246H mutant. The pH profile of D144V/F246H (Fig. 2B, blue) overlapped with that of D144V/L244H within the pH range investigated. The estimated position of His244 in the D144V/L244H mutant appeared to be further from the heme iron (7.2 Å) than the desired range (5–6 Å) (Fig. 3) [26,27,29], but the possibility that the side-chain of histidine could flip towards heme iron to function as an acid-base catalyst upon binding of H_2O_2 to heme cannot be discounted. The finding that the pH profile was minimally affected by the mutations despite the introduction of histidine into the heme distal pocket clearly suggests that distal side-chains, such as aspartic acid and histidine, do not account for the pH dependence of the dye-decolorizing activity of *Vc*DyP.

Initially, we replaced Asp144 with valine and introduced histidine into the heme distal site (D144V/L244H and D144V/F246H) to avoid catalytic competition. Subsequently, Asp144 was retained to maintain the architecture of the distal heme cavity and histidine introduced into the heme distal pocket in WT *Vc*DyP (L244H or F246H). The shape of the pH profile of dye-decolorization activity for the F246H and L244H mutants resembled that of WT *Vc*DyP, but activity at optimal pH was lower (Supplemental Fig. S3). Therefore, additional histidine at the heme distal site appears to impede dye-decolorizing activity.

In B-type DyP from *Pseudomonas putida*, mutation of Asp136 (corresponding to Asp144 in *Vc*DyP) to asparagine yielded a significant shift in optimal pH of dye decolorization by ~4 pH units [30]. We additionally examined the pH profile of an asparagine mutant at position 144 (D144N *Vc*DyP; Fig. 2B, green). Notably, this mutant was almost inactive over a pH range of 3–10. Absolute activity was ~20-fold lower than that of WT *Vc*DyP, indicating that replacement of the hydroxyl group (–OH) with amino group ($–NH_2$) results in inactivation. The collective results support the theory that the distal residues are not involved in determining pH dependence of the dye-decolorizing activity of *Vc*DyP.

3.2. pH dependence of compound I formation of VcDyP

The finding that the pH profile of the dye-decolorizing activity of *Vc*DyP is not affected by mutation of Asp144 suggests no relation of pH to the reaction of *Vc*DyP with H_2O_2. To examine pH dependence of the reaction with H_2O_2, we compared the rate of compound I formation by reaction of *Vc*DyP with H_2O_2 between pH values of 4.0 and 7.0. Addition of 1 equivalent of H_2O_2 at pH 4.0 led to a decrease in Soret absorbance (Fig. 4, red solid line), accounting for the formation of compound I, similar to that observed for horseradish peroxidase (HRP) and cytochrome *c* peroxidase [31]. The time-course of compound I formation at pH 7.0 (Fig. 4, blue solid line) was comparable to that at pH 4.0. Next, the initial velocity (V_0) of the reaction was plotted against pH (Supplemental Fig. S4). The V_0 value for dye-decolorizing activity was largest at pH 4.5 and smallest at pH 7.5. The maximum value of V_0 at pH 4.5 was 0.60 μM min^{-1}, which was 4.6-fold larger than minimum V_0 at pH 7.5 (0.13 μM min^{-1}). For dye-decolorizing activity, the maximum value at pH 4.5 (16.1 nmol mg^{-1} s^{-1}) was ~30-fold larger than the minimum value at pH 7.0 (0.55 nmol mg^{-1} s^{-1}) (Fig. 2B). The data clearly indicate that reaction of *Vc*DyP with H_2O_2 can produce compound I at any pH. Therefore, formation of compound I does not underlie the pH dependence of the dye-decolorizing activity of *Vc*DyP.

In the reaction of *Vc*DyP with H_2O_2 in the presence of 1 equivalent of RB19, Soret absorbance was regained (Fig. 4, red solid line), indicating that ferric heme is regenerated by abstracting electrons from the substrate. The rate of conversion of compound I to ferric heme at pH 7.0 was significantly slower than that at pH 4.0 (Fig. 4, blue solid line). Compound I of *Vc*DyP converted to ferric heme without RB19 at both pH 4.0 and 7.0 (Fig. 4, dashed lines), which was comparable to that in the presence of RB19 at pH 7.0. These results suggest that electrons are not derived from RB19 at pH 7.0, but acquired from an unknown source. Accordingly, we propose that the lower dye-decolorizing activity at neutral pH is caused by slow radical transfer from heme to the substrate, but not by reaction of H_2O_2 with heme to form compound I.

3.3. Involvement of His178 in pH-dependent dye-decolorizing activity

As discussed previously [3,12,14,32,33], the heme binding pocket is not considered the active site of the dye-decolorizing reaction, in view of the lack of space for bulky dye compounds near the heme. Data from mutational analyses suggest that the active site of dye decolorization involves Tyr129 and Tyr235, which are located at a dimer interface ~18 Å apart from the heme iron (Supplemental Fig. S5) [3]. For reaction with bulky substrates at the surface active site, radicals generated by the reaction of heme with H_2O_2 need to be transferred to this location. Indeed, formation of protein surface radicals has been reported in other DyPs [13,14,33–35]. In contrast, small compounds, such as guaiacol, can access heme without requiring long-range radical transfer. This clear difference between dye decolorization and peroxidase reactions using guaiacol as a substrate leads to distinct pH dependence.

Previously, two histidine residues (His178 and His242) located near heme (Supplemental Fig. S6) were individually mutated to leucine (H178L, H242L) and dye-decolorizing activities evaluated [3]. The H242L mutant retained activity, indicating that this residue is not involved in radical transfer to the active site. However, the H178L mutant was considerably less active in dye decolorization although its guaiacol oxidation activity was similar to that of WT *Vc*DyP. Accordingly, His178 is proposed as one of the residues that determines the radical transfer pathway from heme to the active site. Here, we constructed three mutants in which His at position 178 was substituted with aromatic residues, such as phenylalanine (H178F), tyrosine (H178Y) and tryptophan (H178W).

With the expectation that the bulky side-chain introduced near heme would prevent binding of heme to the protein, we measured absorption spectra of all three His178 mutants. Although a small shoulder was present at ~388 nm, the spectra were characteristic of 5-coordinate high-spin heme as observed for the WT enzyme (Supplemental Fig. S1B), indicative of proper heme binding to these mutant proteins. Furthermore, CD spectra of the His178 mutants were similar to that of the WT enzyme (Supplemental Fig. S2), suggesting that introduction of the bulky

side-chain had a minimal effect on the protein structure. The pH profiles of dye-decolorizing activity of the three His178 mutants are shown in Fig. 5. The activities of H178Y and H178W mutants at pH 4.5 were 3–5% that of WT *Vc*DyP (Fig. 5). Upon elevation to pH 7.0, a slight increase in activity was observed. However, considering the experimental errors, these changes were not significant.

In contrast to H178Y and H178W mutants, the dye decolorization activity of the H178F mutant at pH 4.5 was ~35% that of WT *Vc*DyP (Fig. 5) [3] but considerably higher than that of the H178L mutant (<1% of WT *Vc*DyP) [3], indicating that the presence of an aromatic group at position 178 facilitates catalytic activity. Although phenylalanine is fairly resistant to ring oxidation compared with tyrosine and tryptophan, a radical transfer pathway including three phenylalanine residues has been reported for DyP from fungus *Auricularia auricula-judae* [36]. Tryptophan or tyrosine radicals generated at position 178 may be stable and unsuitable for dye degradation while Phe178 facilitates radical transfer from heme to Tyr109. The shape of the pH profile of the H178F mutant was similar to that of WT *Vc*DyP, with maximum activity at pH ~4 (Fig. 5).

3.4. Role of hydrogen bond of His178 in radical transfer

The crystal structure of *Vc*DyP showed that His178 is positioned within hydrogen bonding distance of Thr277 (2.9 Å) and Asp138 (3.1 Å) (Fig. 6). To confirm whether hydrogen bonds of His178 contribute to the pH profile of dye decolorization, we replaced Thr277 or Asp138 with valine (T277V or D138V). Although the maximum specific activity of the T277V mutant was approximately half that of WT *Vc*DyP, its pH profile for dye decolorizing activity was similar, with maximal activity at pH 4.0-4.5 (Fig. 7), indicating no shift in the optimal pH value of dye-decolorizing activity. These enzymatic characteristics were similar to those observed for the H178F mutant (Fig. 5).

The pH profile of dye-decolorizing activity of the D138V mutant is presented in Fig. 7.

Although the specific activity of this mutant at pH 3–5 was significantly lower than that of WT enzyme, maximal activity was observed at pH 6.5. Lower activity at acidic pH may be partly due to partial denaturation during measurements. The specific activity of the D138V mutant at pH 6.5 was 5.2 nmol mg^{-1} s^{-1}, which was approximately a third that of WT enzyme at pH 4.5. Stopped-flow experiments also showed dye-decolorization activity at pH 7.0 but loss of activity at pH 4.0 (Supplemental Fig. S7A). Since the radical transfer step from heme to RB19 is significantly slower than compound I formation (Fig. 4), radical transfer is accelerated in the D138V mutant at pH 6.5, indicating that the hydrogen bond between Asp138 and His178 is essential for radical transfer to the active site at low pH. Interestingly, V_0 of compound I formation was optimal at pH 4.0 (Supplemental Fig. S7B), suggesting that the radical transfer pathway, but not radical formation, contributes the shift in optical pH of dye-decolorizing activity of the D138V mutant. While His178 forms hydrogen bonds with both Asp138 and Thr277, the results obtained with T277V and D138V mutants indicate that only the hydrogen bond between His178 and Asp138 is essential for dye-decolorizing activity. Since the pK_a of the side-chain of aspartic acid is ~4, protonation of Asp138 would affect the hydrogen bond status between His178 and Asp138. Based on the collective results, we conclude that the pK_a of the side-chain of aspartic acid at position 138, and not distal Asp144, is responsible for pH dependence of the dye-decolorizing activity of *Vc*DyP.

4. Discussion

4.1. Effect of a distal charged residue on pH-dependent dye-decolorizing activity

Previously, we showed that substitution of Asp144 with valine led to almost complete loss of dye-decolorization activity [3], supporting the requirement of the distal aspartic acid for dye decolorization. The optimal pH of 4.5 for dye-decolorizing activity of *Vc*DyP additionally supports a role of aspartic acid as an acid-base catalyst [3]. Contribution of an acidic residue in the heme distal site to the peroxidase reaction has also been demonstrated in CPO, which lacks

a well-conserved distal histidine, unlike most other heme peroxidases. Instead, glutamic acid (pK_a 4.3) is present at the corresponding position in most peroxidases [23]. The optimum pH of CPO for peroxidase activity is <4 [20,37], distinct from other heme peroxidases, but close to pK_a of the side-chain of glutamic acid [38,39]. Therefore, the glutamic acid residue of CPO is assumed to be an acid-base catalyst, which abstracts a proton from H_2O_2 and transfers it to the terminal oxygen of the hydroperoxy species to facilitate cleavage of the O-O bond [23,40,41]. In contrast, the pH profile of guaiacol oxidation shows that HRP is most active at pH ~6.0, corresponding to pK_a of the side-chain of histidine [42]. Considering that mutation of Asp144 in *Vc*DyP to valine leads to complete loss of DyP activity [3], we presumed that Asp144 acts as an acid-base catalyst as reported in CPO.

To examine this theory, we substituted Asp144 with histidine with a higher pK_a, with the aim of shifting the optimal pH towards neutral. However, replacement of Asp144 with histidine induced a marked decrease in dye-decolorization activity at pH 4.0 and 7.0 (Fig. 2A), indicating that the introduced histidine does not function as a catalyst. This result was consistent with data obtained for DyP from *Enterobacter lignolyticus* [43]. Inactivation of the D144H mutant *Vc*DyP may be attributable to the location of His144, since the distance between distal histidine and heme iron is reported to be related to peroxidase and peroxygenase activities [25–27,29]. Although myoglobin and hemoglobin have distal histidine hydrogen bonds to heme-bound O_2, their peroxidase activities are significantly lower than that of peroxidase. The distance between Nε of the distal histidine (His64 for myoglobin) and proximal oxygen of iron-bound dioxygen is 2.7 Å [28], which is shorter (3.9 Å) than that of most peroxidases [44]. When the position of the distal histidine was removed slightly further from heme via replacement of His64 with leucine and Phe43 with histidine (F43H/H64L myoglobin mutant), the distance between Nε of distal histidine (His43) and heme iron was altered to 5.7 Å [45], equivalent to that of cytochrome *c* peroxidase (5.6 Å) [25,46]. The guaiacol oxidation rate of F43H/H64L myoglobin was 6.5-fold larger than that of WT myoglobin [25]. In contrast, when histidine was removed

further from heme as a result of replacing Leu29 instead of Phe43 with histidine (L29H/H64L myoglobin), the distance was calculated as 6.6 Å [25] and guaiacol oxidation rate was ~30% that of WT myoglobin [25]. These results imply that location of the distal histidine in the heme pocket is important for function as an acid-base catalyst.

In the D144H mutant, the distance between Nε of His144 and heme iron was estimated as 4.1 Å (Fig. 3A), comparable to that between distal histidine and heme in myoglobin [28], which coincided with almost complete loss of activity (Fig. 2A). In contrast, the distances for D144V/L244H and D144V/F246H mutants were estimated as 7.2 and 5.4 Å, respectively (Fig. 3B, C). The activities of both mutants were markedly higher than that of D144V although both were ~25% relative to WT *Vc*DyP. These results further support the theory that the distal histidine position is critical for enzymatic activity of *Vc*DyP.

As described above, pH dependence of the dye-decolorizing activity of the D144V/L244H and D144V/F246H mutants was indistinguishable from that of WT *Vc*DyP (Fig. 2B), suggesting that pK_a of the side-chain of histidine does not contribute to pH dependence. Therefore, charged residues, such as histidine and aspartic acid, in the distal pocket do not present a decisive factor for the pH dependence of dye decolorization by *Vc*DyP. This conclusion is not unexpected, since although H_2O_2-dependent dye decolorization does not occur in WT *Vc*DyP at neutral pH, the enzyme itself reacts with H_2O_2 (Fig. 4) and a covalent bond is formed between Tyr109 and Tyr133 [3]. The non-significant differences in compound I formation rate between pH 4.0 and 7.0 (Fig. 4) supports the following hypothesis: compound I of *Vc*DyP is formed at any pH, but the radical formed at heme is not efficiently transferred to the surface active site at neutral pH.

Interestingly, the distal aspartic acid is almost completely conserved but plays different roles among the multiple DyP types [4,16]. Upon mutation of the distal aspartic acid of A-type DyP from *E. coli* to asparagine, guaiacol oxidation activity was retained at a similar level as WT

enzyme [47]. In contrast, substitution of the distal aspartic acid of D-type DyP from *Thermomonospora curvata* led to significant loss of activity (by $<10^{-3}$-fold), indicative of acid-base catalyst function [48]. Modest changes were observed in a number of B-type DyPs upon replacing the distal aspartic acid. The k_{cat} value of the ABTS oxidation reaction of the Asp mutant of B-type DyP from *Rhodococcus jostii* RHA1 was half that of WT enzyme [49]. Thus, there is no consensus regarding the specific role of distal residues in the enzymatic activity of DyPs. Based on our findings, we conclude that distal aspartic acid is not a determinant of the pH dependence of dye decolorization.

4.2. Alterations in the radical transfer pathway

Next, we focused on the radical transfer pathways. His178, which is located 3.3 Å (closest distance) apart from the edge of heme (Fig. 6), is a potential factor contributing to the pH dependence of the dye-decolorizing activity of *Vc*DyP [3]. In a previous study, we proposed pH-dependent radical transfer from heme to Tyr133/Tyr109 or Tyr129/Tyr235 via His178 (Supplemental Fig. S6) [3]. Radicals transferred to Tyr133 at higher pH are used to form cross-links with Tyr109 from a different subunit while at lower pH, radicals are transferred to Tyr129 and/or Tyr235 to decolorize dyes.

Upon substitution of His178 with aliphatic leucine, dye-decolorizing activity was lost but cross-links were formed, even at lower pH, indicating that radicals move to Tyr133, but not Tyr129/Tyr235 in this mutant [3]. We intended to introduce an aromatic residue at position 178 to fix the radical transfer path to Tyr129/Tyr235, but not Tyr133. In contrast to the H178L mutant [3], the H178F mutant was half as active as WT *Vc*DyP, indicating that an aromatic ring at this position aids in radical transfer from heme for dye decolorization. The pH profile of dye decolorization activity of the H178F mutant was similar to that of WT *Vc*DyP (Fig. 5). Substitution of Asp138 that forms a hydrogen bond with His178 with valine rendered the protein almost inactive at pH 4.0, but more active that the WT enzyme at pH >6.5 (Fig. 7). The

D138V mutant, which was slightly inactive at lower pH, lost ~80% activity upon incubation at 25 °C for 100 s. However, the guaiacol oxidation activity of the mutant at pH 4.0 was significantly higher than that of WT enzyme (Supplemental Fig. S7). These results support the previous proposal that radical transfer from heme to Tyr is controlled by His178; at pH 4.0, radicals generated at the heme of WT *Vc*DyP move to Tyr129/Tyr235 via His178 where dye substrates are decomposed, while at pH 7.0, radicals move to Tyr133 and are consumed to form an intersubunit covalent bond with Tyr109 (Supplemental Fig. S5) [3]. One possible mechanism underlying the pH-dependent switch of the radical transfer pathway is an orientation change of the side-chain of His178 via protonation/deprotonation. In some proteins, charged residues play a role in gating for electron transfer [50–52]. For example, a conformational flip of a side-chain of histidine upon substrate binding in nitrous oxide reductase contributes to gating electron transfer [51]. Such a change would occur in *Vc*DyP.

4.3. pH dependence of the dye-decolorizing activity of VcDyP

The optimal pH for RB19 decolorization by WT *Vc*DyP is 4.5 (Fig. 3). Michaelis-Menten analysis showed that K_m of WT enzyme at pH 4.5 (30 ± 3 μM) was only ~2-fold lower than that at pH 7.0 (66 ± 34 μM) (Table 1), indicating that substrate binding is not a factor underlying low activity at neutral pH. While the change in K_m does not account for enhancement of *Vc*DyP activity at pH ~4, the extremely large k_{cat} may be a contributory factor. Under low pH conditions, the hydrogen bond between His178 and Asp138 is cleaved by protonation of Asp138, causing conformational changes and facilitating radical transfer from heme to Tyr129/Tyr235 rather than Tyr109/Tyr133 (Fig. 8). Minimal changes were observed for the Thr278 mutant (Fig. 7), which also forms a hydrogen bond with His178 (Fig. 6), suggesting that the hydrogen bond between Asp138 and His178 is necessary for dye decolorization by *Vc*DyP, but not that between His178 and Thr278. The optimal pH of the D138V mutant was shifted to pH 6.5. Since aspartic acid with pK_a of side-chain of ~4 is absent in the D138V mutant, the shift in optimal pH toward neutral pH may account for the pK_a of His178 (Fig. 7). Accordingly, we propose that the pK_a of

Asp138, but not Asp144, contributes to pH dependence of the dye-decolorizing activity of WT *Vc*DyP (Fig. 8). Both Asp138 and His178 in *Vc*DyP are conserved in B-type DyPs (Supplemental Fig. S8). Although numerous investigations on the role of distal Asp (Asp144 in the case of *Vc*DyP) in dye-decolorizing activity have been conducted[9,10,43,48,49], no previous reports have focused on the significance of the hydrogen bond between Asp138 and His178. Our findings support a key decisive role of this hydrogen bond in the pH dependence of dye decolorization activity of DyPs.

5. Conclusion

In summary, we have focused on the pH dependence of the dye-decolorizing activity of *Vc*DyP in this study. Asp144 at the heme distal site is necessary for DyP activity but does not contribute to pH dependence. Mutation of Asp138 to valine led to a shift in optimal pH to 6.5 concomitant with ~10-fold higher catalytic efficiency relative to WT *Vc*DyP at pH 4.5. While the detailed mechanisms underlying enhancement of activity at neutral pH remain to be established, we propose that a hydrogen bond between His178 and Asp138 plays a key role in pH-dependent dye-decolorizing activity through inducing alterations in the radical transfer pathway.

Abbreviation List

DyP	dye-decolorizing peroxidase
*Vc*DyP	DyP from *Vibrio cholerae*
RB19	Reactive blue 19
WT	wild-type.

Declaration of competing interest

The authors declare that they have no conflict of interest with the contents of this article.

Acknowledgements

This study was supported in part by Grants-in-Aid for Scientific Research (20K05700, 16K05835 to T.U., and 19H05769 to K.I.) from the Ministry of Culture, Education, Sports, Science, and Technology (MEXT) of Japan.

Appendix A. Supplementary data

Supplementary data to this article can be found online at

References

[1] S.J. Kim, M. Shoda, Decolorization of molasses and a dye by a newly isolated strain of the fungus Geotrichum candidum Dec 1, Biotechnol. Bioeng. 62 (1999) 114–119. doi:10.1002/(SICI)1097-0290(19990105)62:1<114::AID-BIT13>3.0.CO;2-T.

[2] Y. Sugano, K. Sasaki, M. Shoda, cDNA cloning and genetic analysis of a novel decolorizing enzyme, peroxidase gene dyp from Geotrichum candidum Dec 1, J. Biosci. Bioeng. 87 (1999) 411–417. doi:10.1016/S1389-1723(99)80087-5.

[3] T. Uchida, M. Sasaki, Y. Tanaka, K. Ishimori, A dye-decolorizing peroxidase from Vibrio cholerae, Biochemistry. 54 (2015) 6610–6621. doi:10.1021/acs.biochem.5b00952.

[4] T. Yoshida, Y. Sugano, A structural and functional perspective of DyP-type peroxidase family, Arch. Biochem. Biophys. 574 (2015) 49–55. doi:10.1016/j.abb.2015.01.022.

[5] J.N. Roberts, R. Singh, J.C. Grigg, M.E.P. Murphy, T.D.H. Bugg, L.D. Eltis, Characterization of dye-decolorizing peroxidases from Rhodococcus jostii RHA1., Biochemistry. 50 (2011) 5108–5119. doi:10.1021/bi200427h.

[6] A. Santos, S. Mendes, V. Brissos, L.O. Martins, New dye-decolorizing peroxidases from Bacillus subtilis and Pseudomonas putida MET94: towards biotechnological applications, Appl. Microbiol. Biotechnol. 98 (2014) 2053–2065. doi:10.1007/s00253-013-5041-4.

[7] T.L. Poulos, J. Kraut, The stereochemistry of peroxidase catalysis., J. Biol. Chem. 255 (1980) 8199–8205.

[8] J.N. Rodriguez-Lopez, A.T. Smith, R.N. Thorneley, Role of arginine 38 in horseradish peroxidase. A critical residue for substrate binding and catalysis., J. Biol. Chem. 271 (1996) 4023–4030.

[9] Y. Sugano, R. Muramatsu, A. Ichiyanagi, T. Sato, M. Shoda, DyP, a unique dye-decolorizing peroxidase, represents a novel heme peroxidase family: ASP171 replaces

the distal histidine of classical peroxidases., J. Biol. Chem. 282 (2007) 36652–36658. doi:10.1074/jbc.M706996200.

[10] M. Lučić, A.K. Chaplin, T. Moreno-Chicano, F.S.N. Dworkowski, M.T. Wilson, D.A. Svistunenko, M.A. Hough, J.A.R. Worrall, A subtle structural change in the distal haem pocket has a remarkable effect on tuning hydrogen peroxide reactivity in dye decolourising peroxidases from: Streptomyces lividans, Dalt. Trans. 49 (2020) 1620–1636. doi:10.1039/c9dt04583j.

[11] A.K. Chaplin, M.T. Wilson, J.A.R. Worrall, Kinetic characterisation of a dye decolourising peroxidase from Streptomyces lividans: New insight into the mechanism of anthraquinone dye decolourisation, Dalt. Trans. 46 (2017) 9420–9429. doi:10.1039/c7dt01144j.

[12] E. Strittmatter, C. Liers, R. Ullrich, S. Wachter, M. Hofrichter, D.A. Plattner, K. Piontek, First crystal structure of a fungal high-redox potential dye-decolorizing peroxidase substrate interaction sites and long-range electron transfer, J. Biol. Chem. 288 (2013) 4095–4102. doi:10.1074/jbc.M112.400176.

[13] D. Linde, R. Pogni, M. Cañellas, F. Lucas, V. Guallar, M.C. Baratto, A. Sinicropi, V. Sáez-Jiménez, C. Coscolín, A. Romero, F.J. Medrano, F.J. Ruiz-Dueñ;as, A.T. Martínez, Catalytic surface radical in dye-decolorizing peroxidase: A computational, spectroscopic and site-directed mutagenesis study, Biochem. J. 466 (2015) 253–262. doi:10.1042/BJ20141211.

[14] R. Shrestha, X. Chen, K.X. Ramyar, Z. Hayati, E.A. Carlson, S.H. Bossmann, L. Song, B. V. Geisbrecht, P. Li, Identification of surface-exposed protein radicals and a substrate oxidation site in A-class dye-decolorizing peroxidase from Thermomonospora curvata, ACS Catal. 6 (2016) 8036–8047. doi:10.1021/acscatal.6b01952.

[15] E. Fernández-Fueyo, I. Davó-Siguero, D. Almendral, D. Linde, M.C. Baratto, R. Pogni, A. Romero, V. Guallar, A.T. Martínez, Description of a Non-Canonical Mn(II)-Oxidation Site in Peroxidases, ACS Catal. 8 (2018) 8386–8395. doi:10.1021/acscatal.8b02306.

[16] Y. Sugano, DyP-type peroxidases comprise a novel heme peroxidase family, Cell. Mol. Life Sci. 66 (2009) 1387–1403. doi:10.1007/s00018-008-8651-8.

[17] R. Singh, L.D. Eltis, The multihued palette of dye-decolorizing peroxidases, Arch. Biochem. Biophys. 574 (2015) 56–65. doi:10.1016/j.abb.2015.01.014.

[18] S.J. Kim, K. Ishikawa, M. Hirai, M. Shoda, Characteristics of a newly isolated fungus, Geotrichum candidum Dec 1, which decolorizes various dyes, J. Ferment. Bioeng. 79 (1995) 601–607. doi:10.1016/0922-338X(95)94755-G.

[19] D. Voet, J.G. Voet, Biochemistry, 4th ed., John Wiley & Sons, New York, 2011.

[20] X. Yi, A. Conesa, P.J. Punt, L.P. Hager, Examining the role of glutamic acid 183 in chloroperoxidase catalysis., J. Biol. Chem. 278 (2003) 13855–13859. doi:10.1074/jbc.M210906200.

[21] R.F. Beers, I.W. Sizer, A spectrophotometric method for measuring the breakdown of hydrogen peroxide by catalase., J. Biol. Chem. 195 (1952) 133–140.

[22] Y. Sugano, R. Nakano, K. Sasaki, M. Shoda, Efficient heterologous expression in Aspergillus oryzae of a unique dye-decolorizing peroxidase, DyP, of Geotrichum candidum Dec 1., Appl. Environ. Microbiol. 66 (2000) 1754–1758.

[23] M. Sundaramoorthy, J. Terner, T.L. Poulos, The crystal structure of chloroperoxidase: a heme peroxidase–cytochrome P450 functional hybrid., Structure. 3 (1995) 1367–1377. doi:10.1016/S0969-2126(01)00274-X.

[24] P.G. Furtmüller, M. Zederbauer, W. Jantschko, J. Helm, M. Bogner, C. Jakopitsch, C. Obinger, Active site structure and catalytic mechanisms of human peroxidases, Arch. Biochem. Biophys. 445 (2006) 199–213. doi:10.1016/j.abb.2005.09.017.

[25] T. Matsui, S. Ozaki, E. Liong, G.N. Phillips, Y. Watanabe, Effects of the location of distal histidine in the reaction of myoglobin with hydrogen peroxide, J. Biol. Chem. 274 (1999) 2838–2844. doi:10.1074/jbc.274.5.2838.

[26] S. Ozaki, T. Matsui, Y. Watanabe, Conversion of myoglobin into a peroxygenease: A catalytic intermediate of sulfoxidation and epoxidation by the F43H/H64L mutant, J. Am. Chem. Soc. 119 (1997) 6666–6667. doi:10.1021/ja970453c.

[27] S. Ozaki, T. Matsui, Y. Watanabe, Conversion of myoglobin into a highly stereospecific peroxygenase by the L29H/H64L mutation, J. Am. Chem. Soc. 118 (1996) 9784–9785. doi:10.1021/ja961223l.

[28] S.E. Phillips, Structure and refinement of oxymyoglobin at 1.6 Å resolution., J. Mol. Biol. 142 (1980) 531–554.

[29] S. Ozaki, M.P.P. Roach, T. Matsui, Y. Watanabe, Investigations of the roles of the distal heme environment and the proximal heme iron ligand in peroxide activation by heme enzymes via molecular engineering of myoglobin, Acc. Chem. Res. 34 (2001) 818–825. doi:10.1021/ar9502590.

[30] S. Mendes, V. Brissos, A. Gabriel, T. Catarino, D.L. Turner, S. Todorovic, L.O. Martins, An integrated view of redox and catalytic properties of B-type PpDyP from Pseudomonas putida MET94 and its distal variants, Arch. Biochem. Biophys. 574 (2015) 99–107. doi:10.1016/j.abb.2015.03.009.

[31] B.H. Dunford, Heme Peroxidases, Wiley-VCH, New York, 1999.

[32] M.C. Baratto, A. Sinicropi, D. Linde, V. Sáez-Jiménez, L. Sorace, F.J. Ruiz-Duenas, A.T. Martinez, R. Basosi, R. Pogni, Redox-Active Sites in Auricularia auricula-judae Dye-Decolorizing Peroxidase and Several Directed Variants: A Multifrequency EPR Study, J. Phys. Chem. B. 119 (2015) 13583–13592. doi:10.1021/acs.jpcb.5b02961.

[33] A.K. Chaplin, T.M. Chicano, B. V. Hampshire, M.T. Wilson, M.A. Hough, D.A. Svistunenko, J.A.R. Worrall, An aromatic dyad motif in dye decolourising peroxidases has implications for free radical formation and catalysis, Chem. - A Eur. J. 25 (2019) 6141–6153. doi:10.1002/chem.201806290.

[34] E. Strittmatter, S. Wachter, C. Liers, R. Ullrich, M. Hofrichter, D.A. Plattner, K. Piontek, Radical formation on a conserved tyrosine residue is crucial for DyP activity, Arch. Biochem. Biophys. 537 (2013) 161–167. doi:10.1016/j.abb.2013.07.007.

[35] M.C. Baratto, A. Sinicropi, D. Linde, V. Sáez-Jiménez, L. Sorace, F.J. Ruiz-Duenas, A.T. Martinez, R. Basosi, R. Pogni, Redox-active sites in Auricularia auricula-judae dye-decolorizing peroxidase and several directed variants: A Multifrequency EPR study, J. Phys. Chem. B. 119 (2015) 13583–13592. doi:10.1021/acs.jpcb.5b02961.

[36] E. Strittmatter, K. Serrer, C. Liers, R. Ullrich, M. Hofrichter, K. Piontek, E. Schleicher, D.A. Plattner, The toolbox of Auricularia auricula-judae dye-decolorizing peroxidase - Identification of three new potential substrate-interaction sites, Arch. Biochem. Biophys. 574 (2015) 75–85. doi:10.1016/j.abb.2014.12.016.

[37] K.M. Manoj, L.P. Hager, Chloroperoxidase, a janus enzyme., Biochemistry. 47 (2008) 2997–3003. doi:10.1021/bi7022656.

[38] J.A. Thomas, D.R. Morris, L.P. Hager, Chloroperoxidase. 8. Formation of peroxide and halide complexes and their relation to the mechanism of the halogenation reaction., J. Biol. Chem. 245 (1970) 3135–3142.

[39] J.A. Thomas, D.R. Morris, L.P. Hager, Chloroperoxidase. VII. Classical peroxidatic, catalatic, and halogenating forms of the enzyme., J. Biol. Chem. 245 (1970) 3129–3134.

[40] H.A. Wagenknecht, W.D. Woggon, Identification of intermediates in the catalytic cycle of chloroperoxidase., Chem. Biol. 4 (1997) 367–372. doi:10.1016/S1074-5521(97)90127-7.

[41] M. Sundaramoorthy, J. Terner, T.L. Poulos, Stereochemistry of the chloroperoxidase active site: crystallographic and molecular-modeling studies, Chem. Biol. 5 (1998) 461–473. doi:10.1016/S1074-5521(98)90003-5.

[42] M.I. Savenkova, S.L. Newmyer, P.R. Montellano, Rescue of His-42 -> Ala horseradish peroxidase by a Phe-41 -> His mutation. Engineering of a surrogate catalytic histidine.,

J. Biol. Chem. 271 (1996) 24598–24603.

[43] R. Shrestha, G. Huang, D.A. Meekins, B. V. Geisbrecht, P. Li, Mechanistic insights into dye-decolorizing peroxidase revealed by solvent isotope and viscosity effects, ACS Catal. 7 (2017) 6352–6364. doi:10.1021/acscatal.7b01861.

[44] M.A. Miller, A. Shaw, J. Kraut, 2.2 Å structure of oxy-peroxidase as a model for the transient enzyme: peroxide complex., Nat. Struct. Biol. 1 (1994) 524–531.

[45] D.B. Goodin, D.E. McRee, The Asp-His-Fe triad of cytochrome c peroxidase controls the reduction potential, electronic structure, and coupling of the tryptophan free radical to the heme., Biochemistry. 32 (1993) 3313–3324.

[46] Y. Watanabe, H. Nakajima, T. Ueno, Reactivities of oxo and peroxo intermediates studied by hemoprotein mutants, Acc. Chem. Res. 40 (2007) 554–562. doi:10.1021/ar600046a.

[47] X. Liu, Q. Du, Z. Wang, D. Zhu, Y. Huang, N. Li, T. Wei, S. Xu, L. Gu, Crystal structure and Biochemical features of EfeB/YcdB from Escherichia coli O157: ASP235 plays divergent roles in different enzyme-catalyzed processes, J. Biol. Chem. 286 (2011) 14922–14931. doi:10.1074/jbc.M110.197780.

[48] C. Chen, R. Shrestha, K. Jia, P.F. Gao, B. V. Geisbrecht, S.H. Bossmann, J. Shi, P. Li, Characterization of dye-decolorizing peroxidase (DyP) from Thermomonospora curvata reveals unique catalytic properties of A-type DyPs, J. Biol. Chem. 290 (2015) 23447–23463. doi:10.1074/jbc.M115.658807.

[49] R. Singh, J.C. Grigg, Z. Armstrong, M.E.P. Murphy, L.D. Eltis, Distal heme pocket residues of B-type dye-decolorizing peroxidase: arginine but not aspartate is essential for peroxidase activity., J. Biol. Chem. 287 (2012) 10623–10630. doi:10.1074/jbc.M111.332171.

[50] W. Wang, R.E. Iacob, R.P. Luoh, J.R. Engen, S.J. Lippard, Electron transfer control in soluble methane monooxygenase, J. Am. Chem. Soc. 136 (2014) 9754–9762. doi:10.1021/ja504688z.

[51] L. Zhang, E. Bill, P.M.H. Kroneck, O. Einsle, Histidine-gated proton-coupled electron transfer to the Cu A site of nitrous oxide reductase, J. Am. Chem. Soc. 143 (2021) 830–838. doi:10.1021/jacs.0c10057.

[52] K. Ravichandran, E.C. Minnihan, Q. Lin, K. Yokoyama, A.T. Taguchi, J. Shao, D.G. Nocera, J. Stubbe, Glutamate 350 plays an essential role in conformational gating of long-range radical transport in Escherichia coli Class Ia ribonucleotide reductase, Biochemistry. 56 (2017) 856–868. doi:10.1021/acs.biochem.6b01145.

[53] W.L. DeLano, The PyMOL molecular graphics system, (2002).

Table 1

Kinetic parameters of *Vc*DyP for RB19 decolorization

		RB19		
		K_m	k_{cat}	k_{cat}/K_m
DyP	pH	μM	s^{-1}	s^{-1} μM^{-1}
WT	4.5	30 ± 3	2.3 ± 0.1	0.077 ± 0.011
WT	7.0	66 ± 34	0.014 ± 0.003	2.1 ± (1.5) $\times 10^{-4}$
D138V	4.0	2.9 ± 1.0	0.17 ± 0.02	0.059 ± 0.027
D138V	6.5	0.53 ± 0.23	0.47 ± 0.03	0.89 ± 0.44

Figure legends

Fig. 1. X-ray crystal structure of the local heme environment of *Vc*DyP (PDB ID: 5DE0).

Fig. 2. (A) Time-course of dye-decolorizing reaction by *Vc*DyP. pH dependence of absorbance changes at 595 nm during catalytic activity of WT at pH 4.0, D144H mutant *Vc*DyP with RB19 at pH 4.0 and pH 7.0, D144V/L244H and D144V/F246H mutant *Vc*DyP at pH 4.0. The reaction was initiated by the addition of *Vc*DyP (0.3 μM) to RB19 (40 μM) in the presence of H_2O_2 (0.2 mM) at 25 °C. (B) pH profiles of RB19-decolorizing activities of WT, D144V/L244H, D144V/F246H and D144N mutant *Vc*DyP. The reaction was initiated by the addition of *Vc*DyP (0.3 μM) to RB19 (40 μM) in the presence of H_2O_2 (0.2 mM) at 25 °C.

Fig. 3. Comparison of the heme distal structures of (A) D144H, (B) D144V/L244H and (C) D144V/F246H mutant *Vc*DyP. Model structures were constructed using PyMOL [53].

Fig. 4. Time-course of compound I formation and decay monitored at 406 nm. Reaction of *Vc*DyP (5 μM) with H_2O_2 (5 μM) in the presence of 5 μM RB19 at pH 4.0 (red) and pH 7.0 (blue). Red and blue dashed lines show the time course at pH 4.0 and pH 7.0 in the absence of RB19, respectively.

Fig. 5. pH profiles of RB19-decolorizing activities of WT, H178F, H178W and H178Y mutant *Vc*DyP. The reaction was initiated by the addition of *Vc*DyP (0.3 μM) to RB19 (40 μM) in the presence of H_2O_2 (0.2 mM) at 25 °C.

Fig. 6. Location of Asp138, His178, and Thr277 in *Vc*DyP (PDB 5DE0). Predicted hydrogen bonds are presented in the dotted line.

Fig. 7. pH profiles of RB19-decolorizing activities of WT, D138G D138V and T277V mutant *Vc*DyP. The reaction was initiated by the addition of enzyme (0.3 μM) to RB19 (40 μM) in the presence of H_2O_2 (0.2 mM) at 25 °C.

Fig. 8. Putative pH-dependent radical transfer. At pH 7, radical transfer occurs from heme to Tyr109 or Tyr133 to form an intermolecular covalent bond between tyrosines. At pH 4, radical transfer occurs from heme to Tyr129 and Tyr235 to degrade dye substrate.

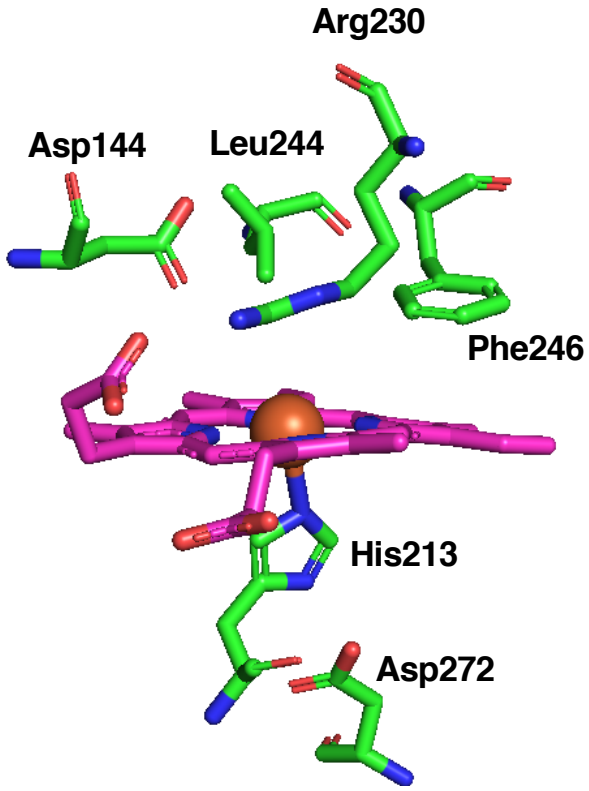

Fig. 1. X-ray crystal structure of the local heme environment of *Vc*DyP (PDB ID: 5DE0)

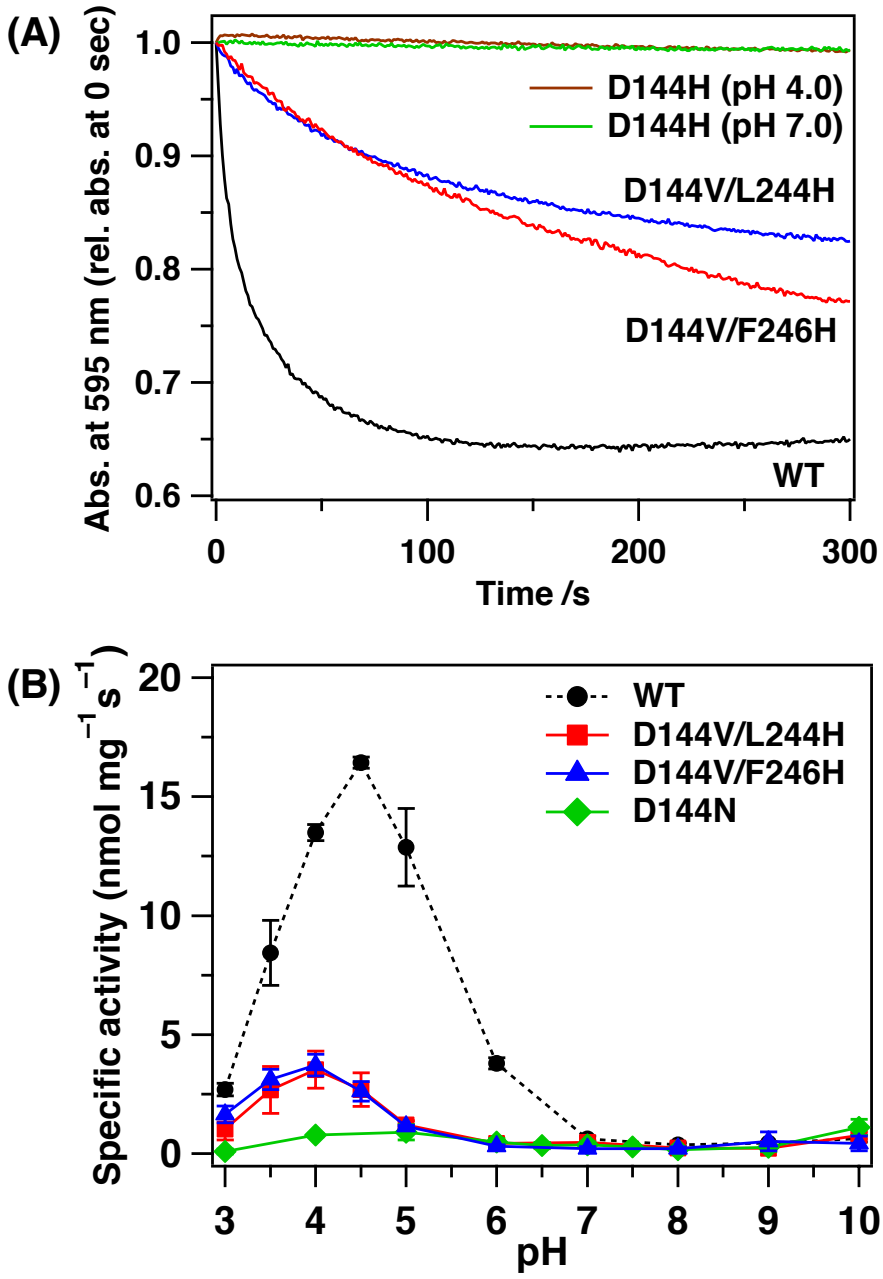

Fig. 2. (A) Time-course of dye-decolorizing reaction by *Vc*DyP. pH dependence of absorbance changes at 595 nm during reaction of WT at pH 4.0, D144H mutant *Vc*DyP with RB19 at pH 4.0 and pH 7.0, D144V/L244H and D144V/F246H mutant *Vc*DyP at pH 4.0. The reaction was initiated by the addition of *Vc*DyP (0.3 μM) to RB19 (40 μM) in the presence of H_2O_2 (0.2 mM) at 25 °C. (B) pH profiles of RB19-decolorizing activities of WT, D144V/L244H, D144V/F246H and D144N mutant *Vc*DyP. The reaction was initiated by the addition of *Vc*DyP (0.3 μM) to RB19 (40 μM) in the presence of H_2O_2 (0.2 mM) at 25 °C.

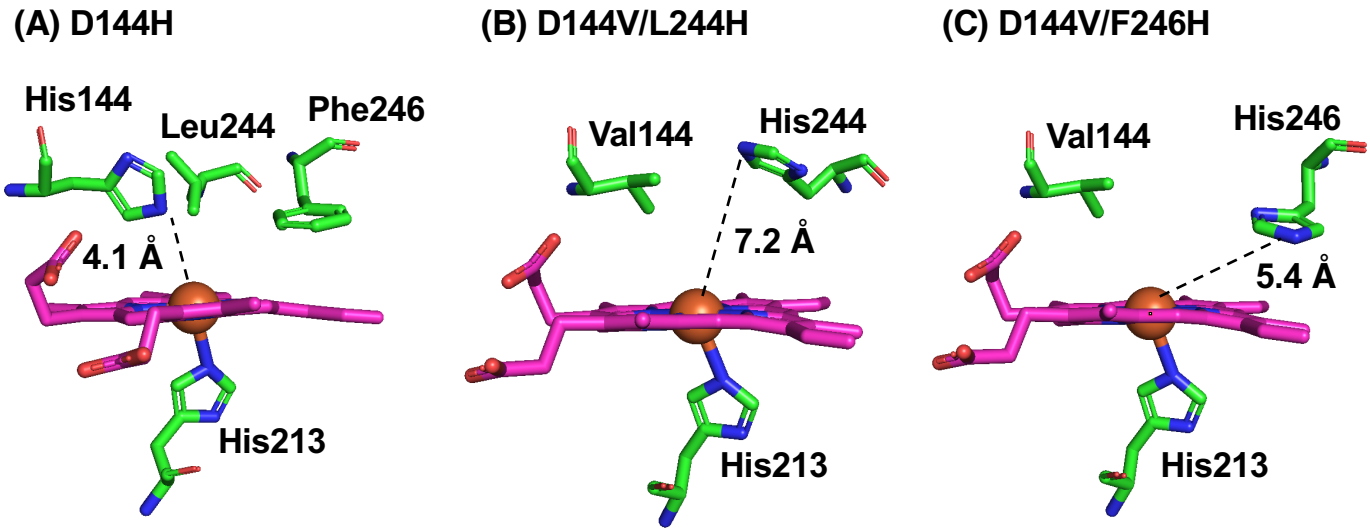

Fig. 3. Comparison of the heme distal structures of (A) D144H, (B) D144V/L244H and (C) D144V/F246H mutant *Vc*DyP. Model structures were constructed using PyMOL [45].

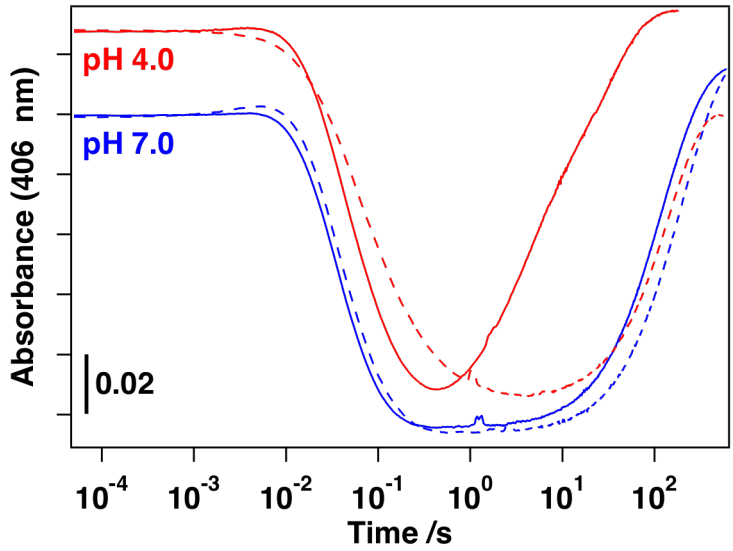

Fig. 4. Time course of compound I formation and decay monitored at 406 nm. Reaction of *Vc*DyP (5 μM) with H_2O_2 (5 μM) in the presence of 5 μM RB19 at pH 4.0 (red) and pH 7.0 (blue). Red and blue dashed lines showed the time course at pH 4.0 and pH 7.0 in the absence of RB19, respectively.

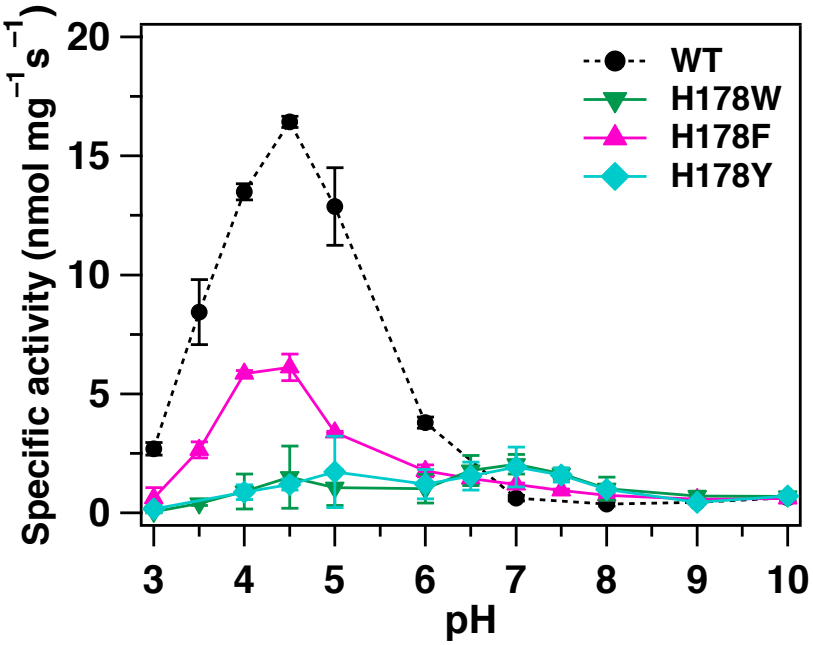

Fig. 5. pH profiles of RB19-decolorizing activities of H178F, H178W and H178Y mutant *Vc*DyP. The reaction was initiated by the addition of *Vc*DyP (0.3 μM) to RB19 (40 μM) in the presence of H_2O_2 (0.2 mM) at 25°C.

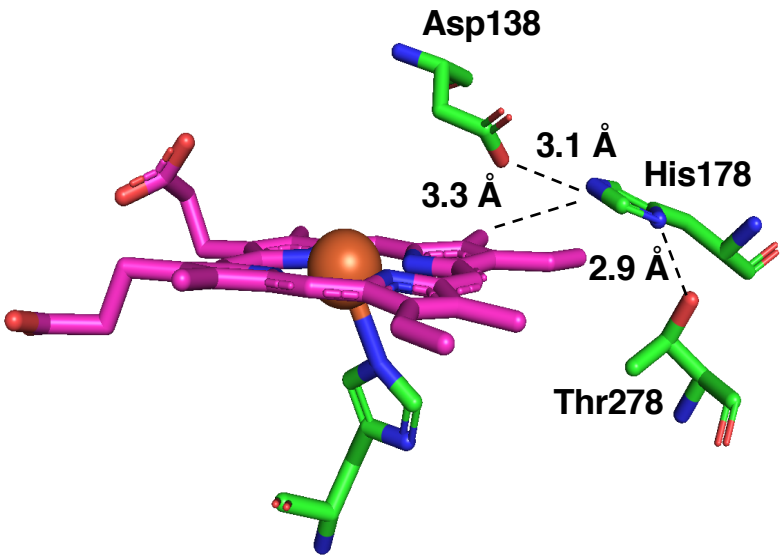

Fig. 6. Location of Asp138, His178, and Thr277 in *Vc*DyP (PDB 5DE0). Predicted hydrogen bonds are shown in dotted line.

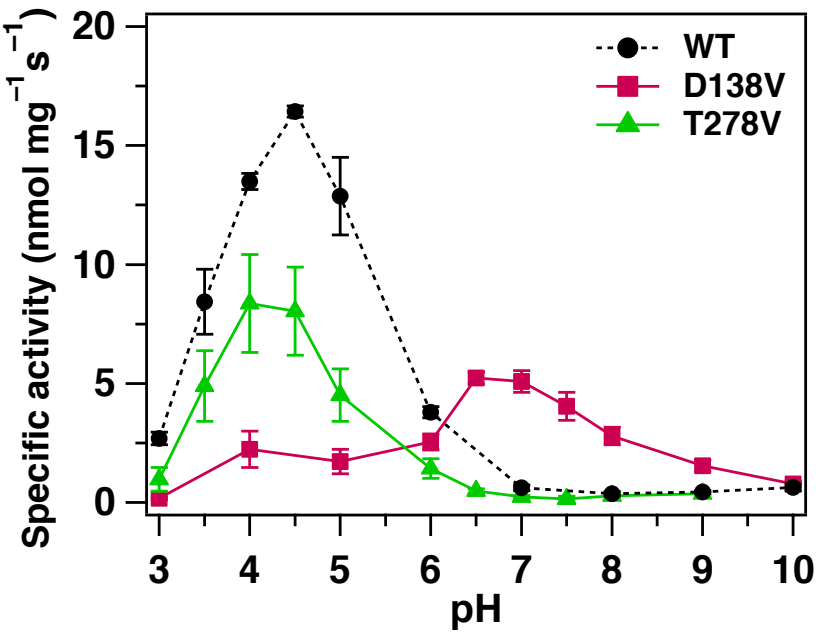

Fig. 7. pH profiles of RB19-decolorizing activities. WT, D138V and T278V mutant *Vc*DyP. The reaction was initiated by the addition of the enzyme (0.3 μM) to RB19 (40 μM) in the presence of H_2O_2 (0.2 mM) at 25°C.

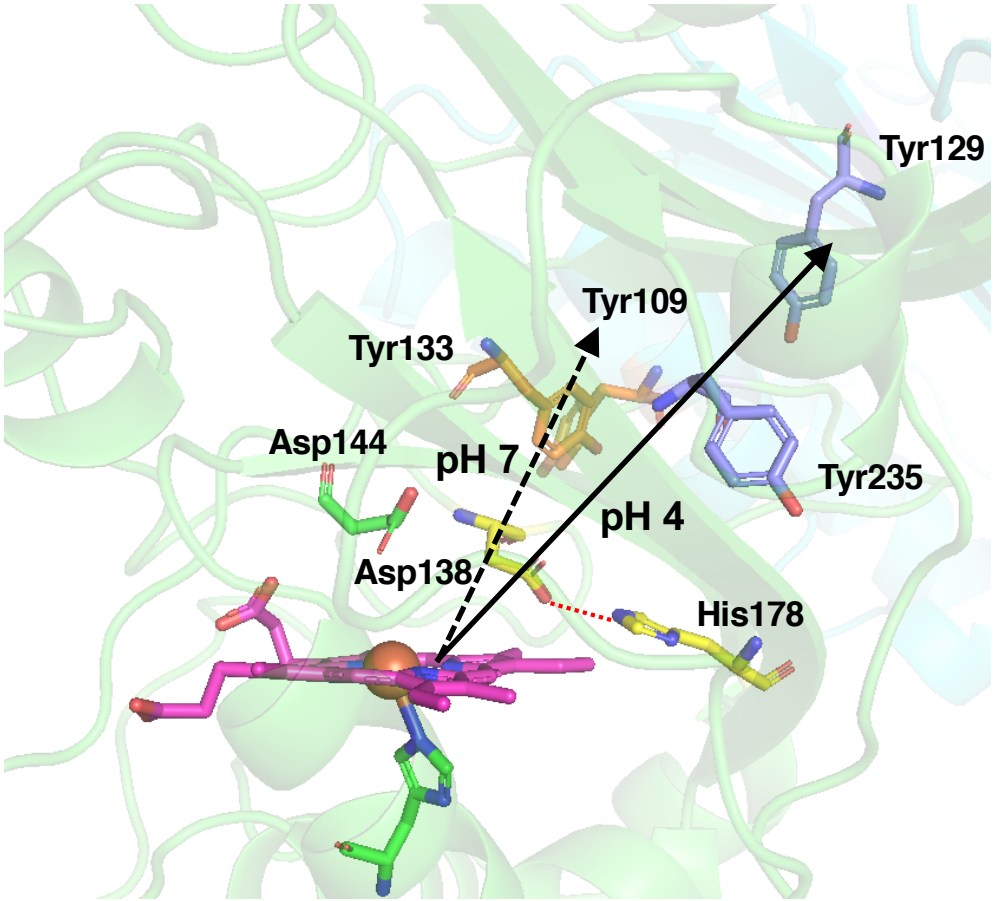

Fig. 8. Putative pH dependent radical transfer. At pH 7, radical transfers from heme to Tyr109 or Tyr133 to form an intermolecular covalent bond between tyrosines. At pH 4, radical transfers from heme to Tyr129 and Tyr235 to degrade dye substrate.

Supplementary Information

Radical transfer but not heme distal residues is essential for pH dependence of dye-decolorizing activity of peroxidase from *Vibrio cholerae*

Takeshi Uchida,*[a,b] Issei Omura,[b] Sayaka Umetsu,[b] and Koichiro Ishimori[a,b]

[a]Department of Chemistry, Faculty of Science, Hokkaido University, Sapporo 060-0810, Japan

[b]Graduate School of Chemical Sciences and Engineering, Hokkaido University, Sapporo 060-8628, Japan

*To whom correspondence should be addressed: Takeshi Uchida,
Phone/Fax: +81-11-706-3501. E-mail: uchida@sci.hokudai.ac.jp

Keywords: heme enzyme, peroxidase, reaction mechanism, *Vibrio cholerae*

Table S1

Oligonucleotides used for construction of expression vectors for mutants. The underlined bases signify the introduced mutations.

Mutants	Primers (up, sense; bottom, anti-sense)
D138V	5'-GCACGTGTGATGACGGGCTTTATTGA-3'
	5'-CGTCATCACACGTGCGTCTAAATAAC-3'
D144H	5'-TTTATTCACGGCACAGAAAACCCGAAAG-3'
	5'-TGTGCCGTGAATAAAGCCCGTCATGTC-3'
D144N	5'-CTTTATTAATGGCACAGAAAACCCGA-3'
	5'-TGTGCCATTAATAAAGCCCGTCATGTC-3'
H178F	5'-TTTGTGTTCAATTTGCCGGCGTGGAATC-3'
	5'-CAAATTGAACACAAAGCGTTGTACCATC-3'
H178W	5'-TTTGTGTGGAATTTGCCGGCGTGGAATC-3'
	5'-CAAATTCCACACAAAGCGTTGTACCATC-3'
H178Y	5'-TTTGTGTATAATTTGCCGGCGTGGA-3'
	5'-CAAATTATACACAAAGCGTTGTACCATC-3'

Table S2

Summary of mutation on the optimal pH and activity.

*Vc*DyP	location	optimal pH	relative activity [a]
WT	–	4.5	1
D144N	distal site	10.0	0.07
D144V/L244H	distal site	4.0	0.21
D144V/F246H	distal site	4.0	0.23
H178F	radical pathway	4.5	0.37
H178W	radical pathway	7.0	0.12
H178Y	radical pathway	7.0	0.12
D138V	H-bond to His178	6.5	0.32
T277V	H-bond to His178	4.0	0.51
L244H	distal site	4.0	0.69
F246H	distal site	4.5	0.18

[a]Relative activity was calculated by dividing the specific activity of the mutants at optimal pH by that of WT *Vc*DyP at pH 4.5.

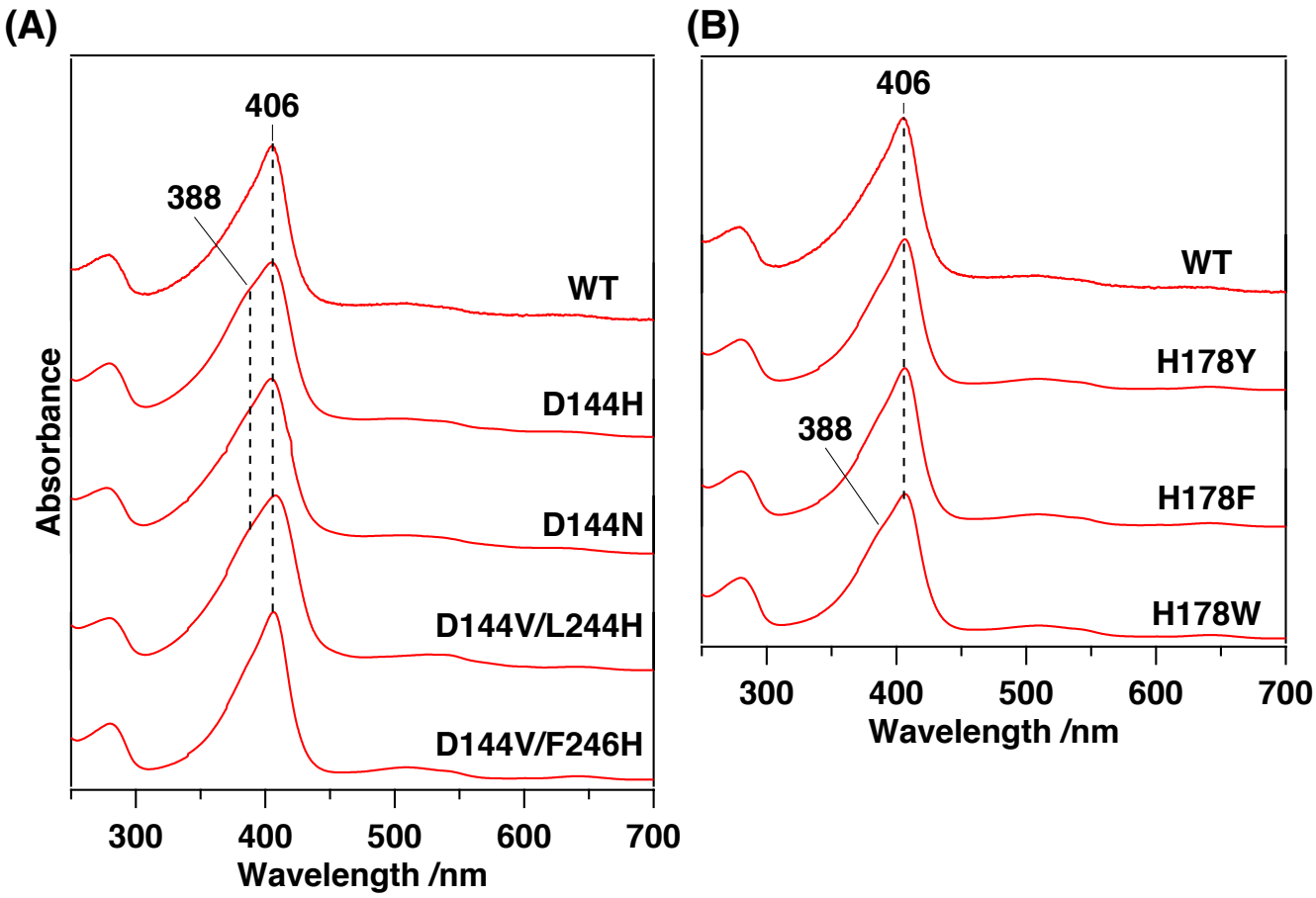

Fig. S1. UV-vis absorption spectra. (A) WT, D144H, D144V/L244H and D144V/F246H mutant *Vc*DyP. (B) WT, H178Y, H178F and H178W mutant *Vc*DyP in 50 mM Tris-HCl and 150 mM NaCl (pH 8.0).

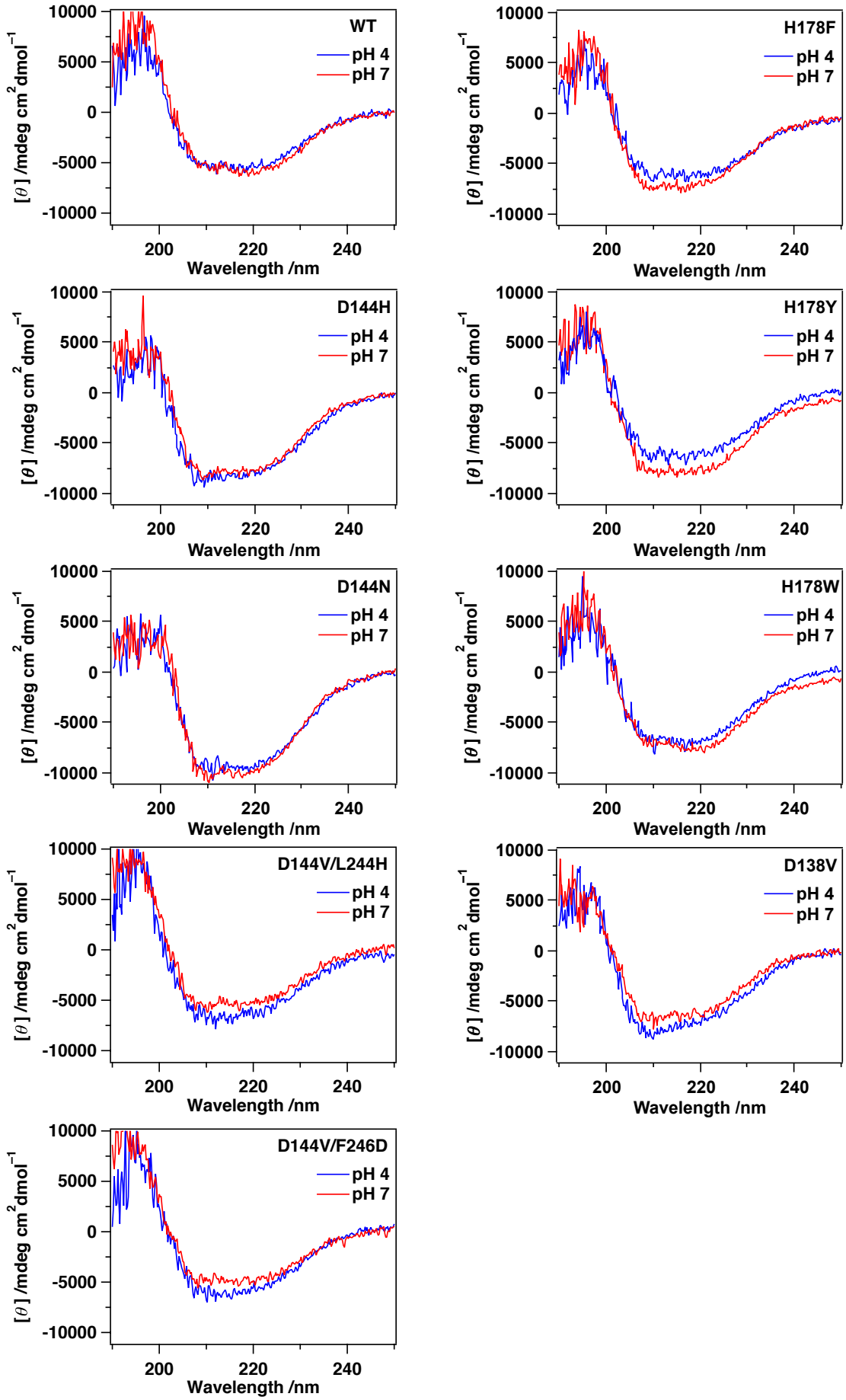

Fig. S2. CD spectra in the far-UV region of WT and mutant DyPs at pH 4.0 and pH 7.0. Circular dichroism (CD) spectra were measured using a Jasco J-1500 CD spectrometer over the spectral range 190−250 nm using a quartz cell with a path length of 0.2 mm at room temperature. The sample was diluted to a final concentration of 30 μM in 25 mM citrate (pH 4.0) or 50 mM sodium phosphate (pH 7.0).

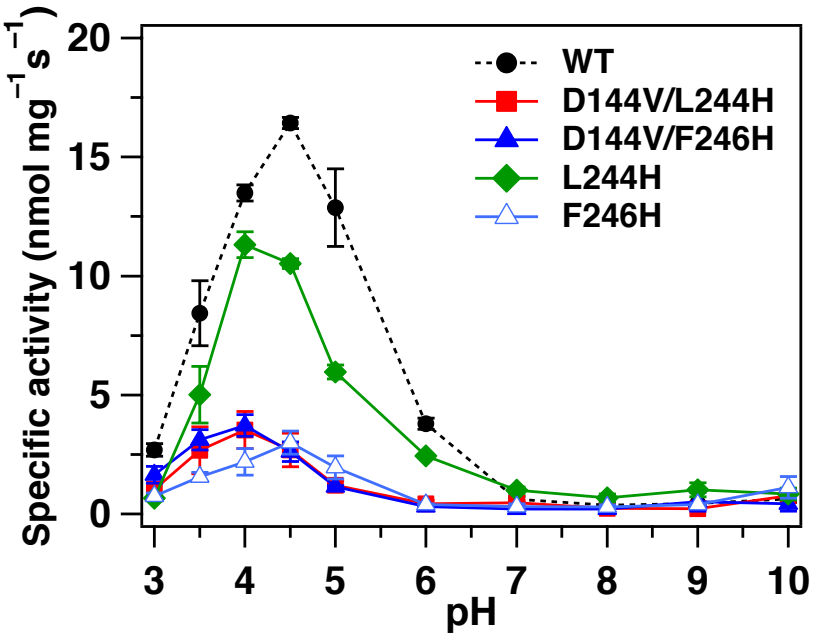

Fig. S3. pH profiles of RB19 degradation activity of WT, D144V/L244H, D144V/F246H, L244H, and F246H mutant *Vc*DyP. The reaction was initiated by the addition of *Vc*DyP (0.3 μM) to RB19 (40 μM) in the presence of H_2O_2 (0.2 mM) at 25 °C.

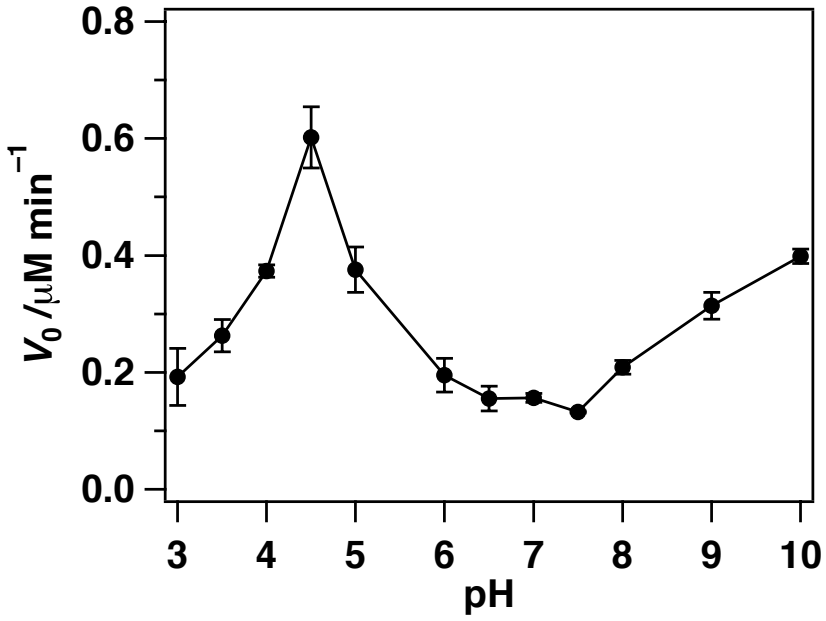

Fig. S4. pH profiles of guaiacol activity of WT *Vc*DyP. *Vc*DyP (0.3 μM) was reacted with 40 μM guaiacol and 0.2 mM H_2O_2 at 25°C.

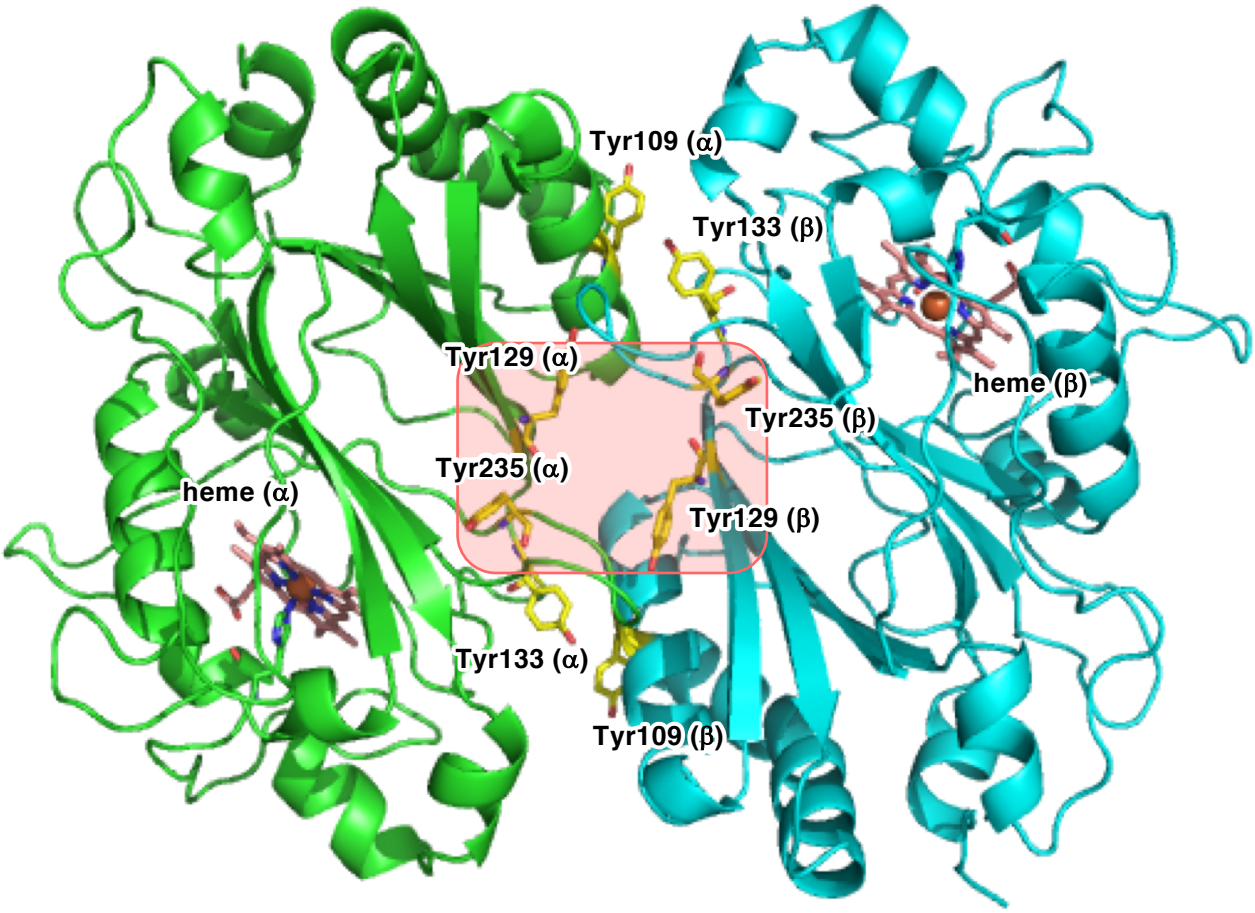

Fig. S5. Location of four reactive tyrosine residues at the dimer interface of *Vc*DyP (PDB ID: 5DE0). Heme is also shown. Putative active site of dye decolorization is shown in red box.

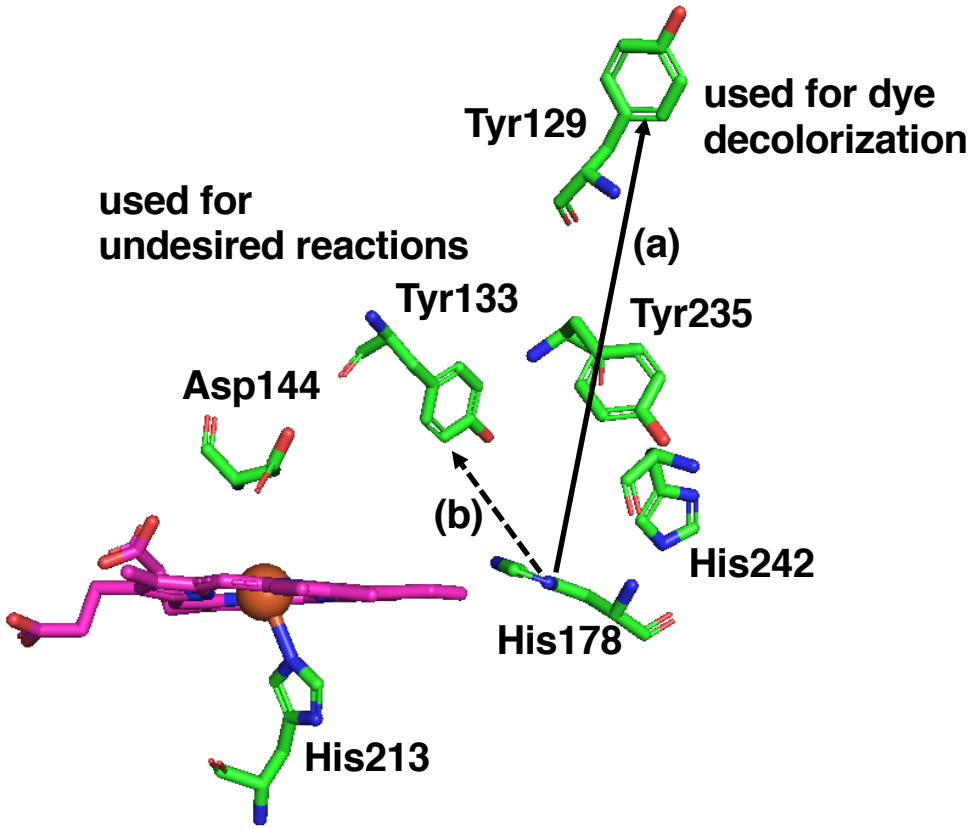

Fig. S6. Location of the residues involved in dye-decolorizing reaction (Asp144, His213, Tyr129 and Tyr235), and covalent bond formation (Tyr133) in *Vc*DyP (PDB 5DE0). Polar residues present near heme (His178 and His242) were also shown. Putative pH-dependent radical transfer pathway at lower pH (a) and higher pH (b)

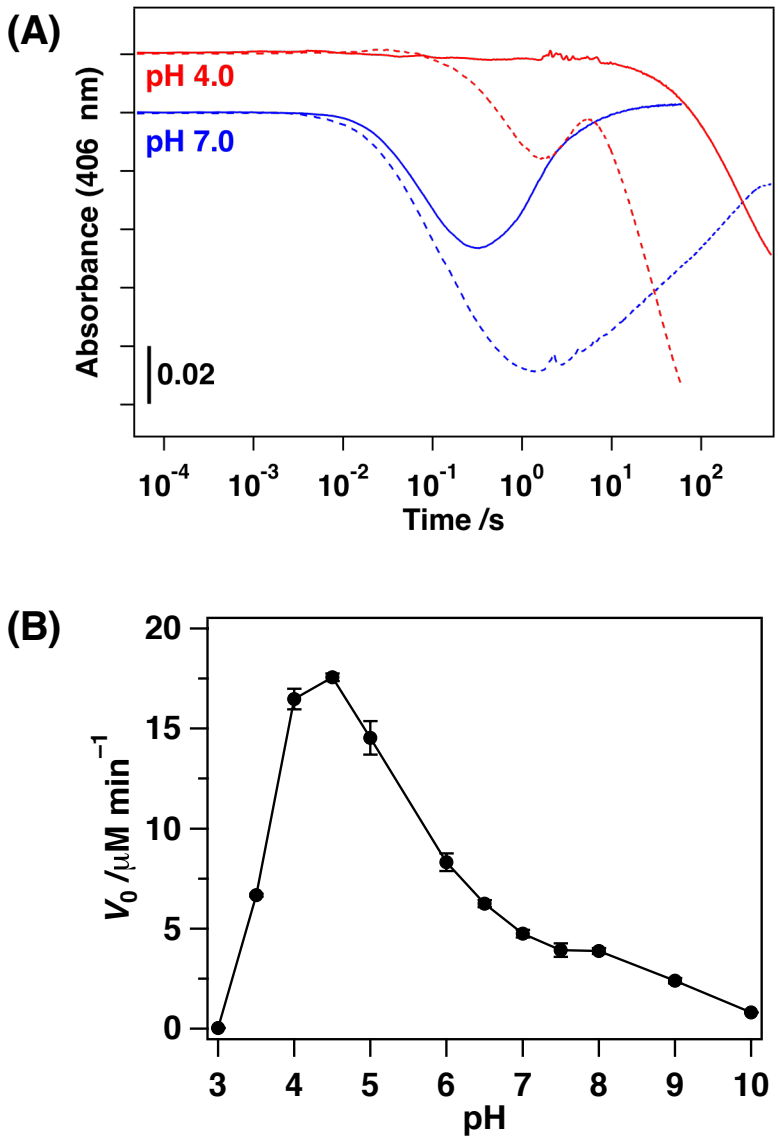

Fig. S7. (A) Time course of compound I formation and decay monitored at 406 nm. Reaction of D138V mutant *Vc*DyP (5 μM) with H_2O_2 (5 μM) in the presence of 5 μM RB19 at pH 4.0 (red) and pH 7.0 (blue). Red and blue dashed lines showed the time course at pH 4.0 and pH 7.0 in the absence of RB19, respectively. (B) pH profiles of guaiacol activity of the D138V mutant *Vc*DyP. *Vc*DyP (0.3 μM) was reacted with 40 μM guaiacol and 0.2 mM H_2O_2 at 25 °C

```
YfeX        --------MSQVQSGILPEHCRAAIWIEANVKGEVDALRAASKTFADKLATFEAKFPDAH
ElDyP       --------MSQVQSGILPEHCRAAIWIEANVKGDVNALRECSKVFADKLAGFEAQFPDAH
VcDyP       --------MFKSQTAILPEAGPFALYTLLKVRQNHAHVLQALKALPALVEEINQNQPGAE
RjDyp       MPGPVARLAPQAVLTPPSAASLFLVLVAGDSDDDRATVCDVISGIDGPLKAVGFRELAGS
PpDyP       ----------MIDGGNMSAAQPGILTPIPVVGRYLFFSISQPEQVAATLASLAAATDGYQ
                             .     :                 . .   :  .

YfeX        LGAVVAFGNNTWRTLSGGVGAEELKDFPGYGKG--LAPTTQFDVLIHILSLRHDVNFSVA
ElDyP       LGAVVAFGHDTWRALSGGVGAEELKDFTPYGKG--LAPATQYDVLIHILSLRHDVNFSVA
VcDyP       LTVSVAFSKGFWSHFEMAS-PPELIDFPELGEGETHAPSTDVDVLIHCHATRHDLLFYTL
RjDyp       LSCVVGVGAQFWDRVSASSKPAHLHPFVPLSGPVHSAPSTPGDLLFHIKAARKDLCFELG
PpDyP       LVVGIGHS----LMLSLGKTVEGMKDYPVLAAPGIDLPSTPSALWCWLRGEDRGEVTLRS
            *   :. .      .. .    :  :   .     *:*   :     .  :.

YfeX        QAAMEAFGDCIEVKEEIHGFRWVEERDLSGFVDGTENPAGEETRREVAVIKDG-VDAGGS
ElDyP       QAAMAAFGDAVEVKEEIHGFRWVEERDLSGFVDGTENPAGEETRREVAVIKDG-VDAGGS
VcDyP       RKGISDIAQDIEIVDETYGFRYLDARDMTGFIDGTENPK-AEKRAEVALVADG-DFAGGS
RjDyp       RQIVSALGSAATVVDEVHGFRYFDSRDLLGFVDGTENPTDDDAADSALIGDEDPDFRGGS
PpDyP       HALERSLAPAFQRTGAVDAFLYGEDRDLSGYKDGTENPKGDAALEAALVSGRGAGLDGGS
            :    :.          .* : : **: *: ******       . :   .    ***

YfeX        YVFVQRWEHNLKQLNRMSVHDQEMMIGRTKEANEEIDGDERPETSHLTR-VDLKEDGKGL
ElDyP       YVFVQRWEHNLKQLNRMSVHDQEMMIGRTKVANEEIDGDERPETSHLTR-VDLKENGKGL
VcDyP       YVMVQRFVHNLPAWNRLNLAAQEKVIGRTKPDSVELEN--VPAASHVGR-VDIKEEGKGL
RjDyp       YVIVQKYLHDMSAWNTLSTEEQERVIGRTKLENVELDDDAQPSNSHVTLNTIVDDDGVEH
PpDyP       FVAVQQWLHDFDRMQAIPGEEMDNIIGRRKSDDEELED--APAYAHVKR-TEQESFEPAA
            :* **:: *::   : :    : :*** *  . *::.   *  :*:   .  ..

YfeX        KIVRQSLPYG-TASGTHGLYFCAYCARLHNIEQQLLSMFG-DTDGKRDAMLRFTKPVTGG
ElDyP       KIVRQSLPYG-TASGTHGLYFCAYCARLYNIEQQLLSMFG-DTDGKRDAMLRFTKPVTGG
VcDyP       KIVRHSLPYG-SVSGDHGLLFIAYCHTLHNFKTMLESMYG-VTDGKTDQLLRFTKAVTGA
RjDyp       DILRDNMAFGSLGEAEYGTYFIGYAKDPAVTELMLRRMFLGEPPGNYDRVLDFSTAATGT
PpDyP       FLLRRGAPWS--DEHRAGLLFAAFGRSFEAFEVQWLRMIG-VEDGVLDGLFRFTRPISGS
            ::* . .::.   .   *  * .:       :     *      *  * :: *: . :*

YfeX        YYFAPSLDKLMAL-----------------------------------
ElDyP       YYFAPSLDKLL-------------------------------------
VcDyP       YFFAPSQVMLQELTLKNQ------------------------------
RjDyp       LFFVPSRDVLESLGDEPAGAESAPEDPVEPAAAGPYDLSLKIGGLKGVSQ
PpDyP       YFWCPPMADGRLDLSALGL----------------------------
             :: *.
```

Fig. S5. Sequence alignment of the B-type DyPs. The alignment was performed using ClustalW2 (http://www.ebi.ac.uk/Tools/msa/clustalw2/). The arginine and histidine corresponding to Asp138 and His178 of *Vc*DyP are shown in red bold type. Proteins used in the alignment are (from top to bottom) YfeX from *Escherichia coli*. *El*DyP (DyP from *Enterobacter lignolyticus*), *Vc*DyP (DyP from *Vibrio cholerae*), *Rj*DyP (DyP from *Rodococcus jostii*), *Pp*DyP (DyP from *Pseudomonas putida*).